Synthesis and Evaluation of ^{18}F-FE-PEO in Rodents: An ^{18}F-Labeled Full Agonist for Opioid Receptor Imaging

Patrick J. Riss[1,2], Young T. Hong[2,3], János Marton[4], Daniele Caprioli[2,5], David J. Williamson[3], Valentina Ferrari[1], Neil Saigal[†2,5], Bryan L. Roth[6], Gjermund Henriksen[7], Tim D. Fryer[2,3], Jeffrey W. Dalley[2,5,8], and Franklin I. Aigbirhio[1,2]

[1]Molecular Imaging Chemistry Laboratory, Wolfson Brain Imaging Centre, Department of Clinical Neurosciences, University of Cambridge, Cambridge, United Kingdom; [2]Behavioural and Clinical Neuroscience Institute, University of Cambridge, Cambridge, United Kingdom; [3]Laboratory for Molecular Imaging, Wolfson Brain Imaging Centre, Department of Clinical Neurosciences, University of Cambridge, Cambridge, United Kingdom; [4]ABX Advanced Biochemical Compounds, Biomedizinische Forschungsreagenzien GmbH, Radeberg, Germany; [5]Department of Psychology, University of Cambridge, Cambridge, United Kingdom; [6]Department of Pharmacology, Division of Chemical Biology and Medicinal Chemistry and NIMH Psychoactive Drug Screening Program, University of North Carolina, Chapel Hill, North Carolina; [7]Petsenteret Norsk Medisinsk Syklotronsenter AS, Oslo, and Institute of Basic Medical Sciences, University of Oslo, Oslo, Norway; and [8]Department of Psychiatry, University of Cambridge, Cambridge, United Kingdom

We have investigated the opioid receptor (OR) agonist (20*R*)-4,5-α-epoxy-6-(2-^{18}F-fluoroethoxy)-3-hydroxy-α,17-dimethyl-α-(2-phenyleth-1-yl)-6,14-ethenomorphinan-7-methanol (^{18}F-FE-PEO) as a candidate OR PET ligand. This tracer is attractive because it combines ^{18}F labeling, is suited to the slow kinetics of high-affinity ligands, and has agonist binding, which has been shown to be more sensitive to changes in OR occupation than is antagonist binding. **Methods:** Agonist potency and off-target binding were investigated in vitro, and autoradiographic studies on rat brain sections were used to assess binding patterns. Quantification of the tracer in vivo was investigated using small-animal PET in rats with blood sampling. **Results:** ^{18}F-FE-PEO was obtained by direct nucleophilic radiofluorination and subsequent deprotection with a yield of 28% ± 15%, a specific activity of 52–224 MBq/nmol, and a radiochemical purity of more than 97% (90 min from end of bombardment). In vitro studies showed it to be a full agonist ligand, which selectively binds to OR with high affinity, although it is not selective to a single OR subtype (inhibition constant, 0.4–1.6 nM across OR subtypes). Autoradiography binding patterns were consistent with the known distribution of OR, although nondisplaceable signal typically constituted one third of the signal in OR-dense regions. Although metabolites were present in blood (~40% of plasma radioactivity was nonparent 3 h after injection), no significant metabolite fraction was found in brain tissue, aiding PET quantification. A plasma input 2-tissue-compartment model provided good fits to the PET data, and regional distribution volumes from the latter correlated well with those from Logan plot analysis (r^2 = 0.98). The cerebellum had the lowest distribution volume, but the time–activity curve data could not be adequately fitted with a 1-tissue-compartment model. Reference tissue models using the cerebellum as the reference region did not provide good fits to the data, so blood-based kinetic analysis is recommended. **Conclusion:** As the first ^{18}F-labeled OR agonist ligand, ^{18}F-FE-PEO is a useful addition to the existing OR ligand portfolio.

Key Words: agonist; FE-PEO; ^{18}F; opioid receptor; PET

J Nucl Med 2013; 54:299–305
DOI: 10.2967/jnumed.112.108688

Opioid receptor (OR) subtypes μ (MOR), δ (DOR), and κ (KOR) belong to the group of G protein–coupled receptors. ORs are prominent targets for imaging studies because opioid signaling pathways are involved with a variety of physiologic functions, including addiction, appetite, cognition, feeding behavior, motivation, pain processing, and social behavior (*1*).

OR binding sites are widely distributed throughout the human brain, with the highest total density being in the amygdala (*2*). Relative expression of the 3 OR subtypes is similar in caudate, putamen, and frontal cortex. In contrast, a few regions show a distinct dominance of a single subtype: thalamus (67% MOR), substantia nigra (66% KOR), and amygdala (60% KOR). OR subtypes are also spatially co-located together in the rat brain (*3–5*); however, relative OR expression levels show varying degrees of agreement between rats and humans. For instance, in the rat, as in humans, MOR dominates in the thalamus and similar levels of the 3 subtypes are found in the striatum, but unlike in humans, in the rat the substantia nigra is dominated by MOR and the amygdala has comparable levels of all OR subtypes.

To date, most validated radioligands available for OR receptor quantification with PET have been antagonists. Their use, however, has limited utility because of the complex nature of opioid neurotransmission. Agonist binding has been shown to be significantly more sensitive to changes in OR occupation than antagonists (*6*); hence, the availability of an OR agonist PET ligand is highly desirable. The ^{11}C-labeled agonist

Received May 17, 2012; revision accepted Aug. 21, 2012.
For correspondence or reprints contact: Patrick J. Riss, Wolfson Brain Imaging Centre, Department of Clinical Neurosciences, University of Cambridge, Box 65, Addenbrooke's Hospital, Cambridge CB2 0QQ, U.K.
E-mail: pr340@wbic.cam.ac.uk
†Deceased.
Published online Jan. 7, 2013

radiotracers ^{11}C-carfentanil, ^{11}C-salvinorin A, and ^{11}C-PEO for OR imaging have been reported and used in humans, nonhuman primates, and rodents, respectively (*7–9*). However, the short half-life of ^{11}C (20.3 min) restricts these compounds to PET centers with a cyclotron and limits quantification in receptor-rich domains with high-affinity radioligands such as ^{11}C-carfentanil and ^{11}C-PEO (*1,10*).

Consequently, we have investigated (20*R*)-4,5-α-epoxy-6-(2-^{18}F-fluoroethoxy)-3-hydroxy-α,17-dimethyl-α-(2-phenyleth-1-yl)-6,14-ethenomorphinan-7-methanol (^{18}F-FE-PEO) as a candidate ^{18}F-labeled OR radiotracer (Fig. 1), with the aim of providing an agonist alternative to the antagonists ^{18}F-cyclofoxy and ^{18}F-fluorethyldiprenorphine (*1,11–14*).

The structural attributes of FE-PEO facilitate the use of structurally matched agonist/antagonist/inverse agonist pairs to study OR occupation and availability in pain management and drug abuse. These investigations have so far been hampered by the lack of available tracers.

MATERIALS AND METHODS

Radiosynthesis

The precursor (TE-TDPEO) was obtained from ABX Advanced Biochemical Compounds and was synthesized as described in Supplemental Figure 1 (supplemental materials are available online only at http://jnm.snmjournals.org). The reference substance (FE-PEO), synthesized from thebaine as described previously (*9*), was also obtained from ABX. Further details on the precursor and reference substance are given in the supplemental data.

^{18}F-FE-PEO was synthesized from TE-TDPEO via aliphatic nucleophilic substitution with [K⊂222][^{18}F]F$^-$ using a TRACERlab FX F-N synthesis module (GE Healthcare) followed by acid hydrolysis of a trityl ether protective group (Supplemental Fig. 16). TE-TDPEO (7.0 ± 0.4 mg) in 0.9 mL of anhydrous MeCN was added to dried [K⊂222][^{18}F]F$^-$ at 40°C. The reaction mixture was heated to 90°C and stirred for 10 min. The reactor was cooled to 40°C before the addition of 1 mL of 1 M HCl in EtOH. After stirring of the mixture at 40°C for 5 min, it was neutralized by adding 1 mL of 1 M NH_4OH.

The obtained mixture was passed through a SepPak plus alumina N cartridge (Waters Ltd.) and injected into the preparative high-performance liquid chromatography (HPLC) system of the FX F-N module. The stationary phase consisted of 2 VWR Chromolith RP-18e columns (10 × 100 mm; Merck KGaA), and the mobile phase was a mixture of MeCN and 0.05 M ammonium formate buffer at pH 6.8 (36:64) at a flow rate of 10 mL/min. The product fraction was collected after a total retention time of 9 min in a vessel containing 50 mL of sterile water. The ultraviolet detection wavelength was 254 nm.

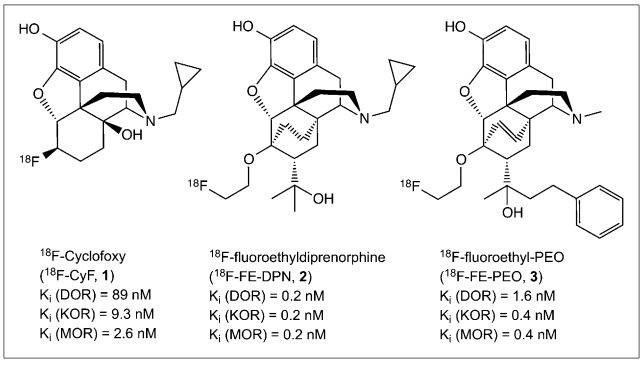

FIGURE 1. ^{18}F-labeled PET ligands for OR imaging.

The diluted product fraction was passed through an Oasis HLB cartridge (Waters Ltd.) preconditioned with 5 mL of ethanol and 10 mL of water. The trapped product was washed with 10 mL of water before the elution of the trapped ^{18}F-FE-PEO in 0.6 mL of ethanol. The ethanolic solution was collected in a vial precharged with 6 mL of 0.9% NaCl solution. The final formulation of ^{18}F-FE-PEO for animal experiments was obtained via sterile filtration of the mixture of ethanol and NaCl solution into a sterile multiinjection vial.

For quality control, 15 μL of the ^{18}F-FE-PEO formulation was injected into an analytic HPLC system (Agilent Technologies U.K. Ltd.). The single radioactive peak eluted after 12–15 min. The specific activity of the product was determined via comparison of the ultraviolet peak area with a calibration curve obtained from 6 different concentrations of FE-PEO in 9% ethanol in water (Supplemental Fig. 17). The identity of ^{18}F-FE-PEO was established by the simultaneous injection of FE-PEO, and radiochemical and chemical purity were determined by integration of the ultraviolet and radioactivity traces, respectively.

Binding Affinity

The potential of FE-PEO to competitively inhibit radioligand binding to a plethora of central nervous system receptors, transporters, and ion channels, stably or transiently transfected in cell culture, was determined as detailed elsewhere (*15*). When a significant inhibition of radioligand uptake was detected at a 10-μM concentration of FE-PEO, the potency of inhibition (inhibitory concentration of 50%) was determined. Inhibition constants (K_i) were computed using the Cheng–Prussof equation (*16*). DOR, KOR, and MOR receptor activation of FE-PEO was measured according to published procedures.

Stability Studies

^{18}F-FE-PEO was mixed with 2.5 mL of heparinized rat blood to obtain a radioactivity concentration of 0.3 MBq/mL of blood, which was distributed into 15 conical tubes (150 μL/tube). The tubes were incubated at 37°C for up to 2 h. After 1, 15, 30, 60, and 120 min, 3 tubes were spun at 5,000 rpm for 5 min before removal of the supernatant plasma (50 μL). Aliquots of the plasma were transferred into 0.3-mL tubes containing acetonitrile (250 μL), and the samples were spun at 5,000 rpm for 5 min. The supernatant was directly spotted on silica gel 60–coated aluminum plates (Merck KGaA) for analysis.

Autoradiography

In vitro autoradiography was conducted following standard procedures detailed previously (*17,18*). Coronal rat brain sections were exposed to ^{18}F-FE-PEO at a concentration of 0.4 nM (~K_i). To assess selectivity for OR receptors, 24 sections from 2 animals were preincubated with either the nonselective OR antagonist naloxone (10 μM; 12 sections) or the MOR-selective agonist [D-Ala^2, *N*-MePhe^4,Gly-ol]-enkephalin (DAMGO) (1 μM; 12 sections). Detection was performed using BAS-IP MS storage phosphor screens (GE Healthcare) and a Duerr CR 35 NDT image plate scanner (Raytest Isotopenmessgeraete GmbH). To quantify the impact of preincubation with naloxone or DAMGO on radioligand binding, regions of interest were drawn on the images using Raytest QWBA software.

PET

All animal experiments were conducted in accordance with the U.K. Animal (Scientific Procedures) Act of 1986. Studies were performed on 3 Lister hooded rats (Charles River). Anesthesia was induced with 2% isoflurane administered in 1 L/min of oxygen and maintained throughout the experiment with less than 1% isoflurane. The left femoral vein was cannulated for intravenous administration of ^{18}F-FE-PEO and drugs, and the left femoral artery was cannulated to allow for collection of blood samples. During all surgical procedures, body temperature was maintained at 37°C using a heating blanket connected to a rectal thermistor probe. After PET imaging, the animals were sacrificed by intravenous injection of 1 mL (200 mg/mL) of pentobarbital sodium, and the brains were harvested for metabolite analysis.

PET data were acquired using a microPET Focus 220 scanner (Concorde Microsystems). The rats were placed prone on the scanner bed, and the head was fixed in a custom-made plastic frame using ear bars and a bite bar. Anesthesia and body temperature were maintained as described above. In addition, oxygen saturation, heart rate, and respiratory rate were measured and maintained within physiologic limits throughout using a noninvasive mouseOX (Starr Life Science Corp.) pulse oximeter sensor attached to the foot.

Before injection, singles-mode transmission data were acquired for 8.5 min using a rotating ^{68}Ge point source (~25 MBq). An attenuation correction sinogram was produced from this scan, and a blank scan of the same duration with scatter correction was applied. In all experiments, ^{18}F-FE-PEO (8–20 MBq) was injected intravenously over 30 s, followed by a 15-s heparinized saline flush. The injected activity was varied in order to keep the injected mass of FE-PEO constant at 0.1 nmol. List-mode data were histogrammed into sinograms for the following time frames: 12×5 s, 6×10 s, 3×20 s, 4×30 s, 5×1 min, 10×2 min, and 30×5 min (3 h in total). Corrections were applied for random events, dead time, normalization, attenuation, scatter, and decay. Fourier rebinning (*19*) was used to compress the 4-dimensional sinograms to 3 dimensions before reconstruction with 2-dimensional filtered backprojection with a Hann window cutoff at the Nyquist frequency. The image voxel size was $0.95 \times 0.95 \times 0.80$ mm, with an array size of $128 \times 128 \times 95$. The reconstructed images were converted to kBq/mL using global and slice factors determined from imaging a uniform phantom filled with an ^{18}F-fluoride solution. This phantom acquisition was also used to cross-calibrate the scanner and the well counter used to measure blood radioactivity concentration.

To determine arterial blood and plasma ^{18}F-FE-PEO kinetics, serial blood samples were taken via the arterial cannula. Blood samples (~30 μL each apart from those used for metabolite analysis) were taken every 6 s for the first 2 min, every 20 s for the next minute, and then at approximately 5, 7, 10, 20, 30, 60, 90, 120, 150, and 180 min. Whole blood and plasma were counted for each sample in a Genie2000 well counter (Harwell Instruments).

Metabolite Analysis

Blood samples collected after 5, 10, 60, 120, and 180 min were used for metabolite studies. Samples of blood (100 μL) were centrifuged at 5,000 rpm for 5 min, and then 50 μL of the supernatant plasma were transferred into 200 mL of methanol, thoroughly agitated, and centrifuged at 5,000 rpm for 5 min. An aliquot (50 μL) of the supernatant was counted, and 20 μL of the supernatant were directly injected into the analytic HPLC system. The HPLC eluate was separated into 2 fractions containing the radioactive metabolites and the intact ^{18}F-FE-PEO, respectively. Both fractions were weighed, and an aliquot of each fraction was counted using a 431-040 well counter (Hidex Oy).

Brain tissue was homogenized by grinding under methanol (3 mL/g of tissue) in a glass tissue homogenizer for 5 min. The supernatant layer was transferred into a centrifuge tube and centrifuged at 5,000 rpm for 5 min. The supernatant was analyzed in the same manner as described for the blood analysis.

PET Data Analysis

For each scan, a mean PET image (1–3 h after injection) was manually coregistered to a T2-weighted MR atlas of 21 healthy Lister hooded rats (*20*), and the dynamic PET images were resliced to the MR atlas using these coregistration parameters. To facilitate the production of regional time–activity curves, the following regions of interest were manually defined on the MR atlas using Analyze 7.0 software (AnalyzeDirect): frontal cortex, striatum, hippocampus, thalamus, amygdala, and cerebellum. The cerebellum was used to produce the reference tissue time–activity curve. For each rat, a Hill function (*21*) was fitted to the blood metabolite data and applied to the plasma input function to produce a metabolite-corrected plasma input function.

Region-of-interest distribution volume (V_T) and nondisplaceable binding potential (BP_{ND}) (*22*) were estimated using a metabolite-corrected plasma input function together with reversible 1-tissue-compartment model (1TCM) and 2-tissue-compartment model (2TCM) and the Logan plot (*23*). Compartmental modeling included blood volume correction using the whole-blood time–activity curve. The results of blood-based modeling were compared with those obtained from the following reference tissue methods: reference tissue model (*24*), simplified reference tissue model (*25*), and reference tissue input Logan plot (*26*), with k_2 of the reference region, as required in the latter method, determined from the 2TCM. Blood and reference tissue compartmental modeling methods (i.e., 1TCM, 2TCM, reference tissue model, and simplified reference tissue model) utilized weighted nonlinear least-squares fitting, with the weights calculated as described by Gunn et al. (*27*). Plasma and reference tissue Logan plots used data acquired 70–180 min after injection. In addition, maps of V_T were produced using the plasma input Logan plot. The correlation between parameters was assessed using Pearson correlation testing.

RESULTS

Radiosynthesis

After some optimization (Supplemental Fig. 18), ^{18}F-FE-PEO was obtained with a reliable yield of 28% ± 15%, a specific activity of 52–224 MBq/nmol, and a radiochemical purity of greater than 97%. To avoid overloading the HPLC column, only 7 mg of labeling precursor were used as a compromise between radiochemical yield and purification of the reaction mixture. The production of the radiotracer took 90 min in total.

Binding Affinity of FE-PEO

FE-PEO did not present significant potency to inhibit binding of radioligands other than for ORs (Table 1). Despite structural modification, FE-PEO retained full agonist characteristics at DOR, KOR, and MOR receptors;

TABLE 1
Central Nervous System Binding Profile of FE-PEO

Binding site	K_i (nM)	Binding site	K_i (nM)	Binding site	K_i (nM)	Binding site	K_i (nM)
5-HT_{1A}	>10,000	α_{1A}	>10,000	D_1	>10,000	KOR	0.4 ± 0.02
5-HT_{1B}	>10,000	α_{1B}	>10,000	D_2	>10,000	M_1	>10,000
5-HT_{1D}	>10,000	α_{1D}	>1,0000	D_3	>10,000	M_2	>10,000
5-HT_{1E}	>10,000	α_{2B}	>10,000	D_4	>10,000	M_3	>10,000
5-HT_{2A}	>10,000	α_{2C}	>10,000	D_5	>10,000	M_4	2,635 ± 420
5-HT_{2B}	>10,000	α_{2D}	>10,000	DAT	>10,000	M_5	>10,000
5-HT_{2C}	>10,000	β_1	>10,000	DOR	1.6 ± 0.2	MOR	0.4 ± 0.03
5-HT_3	>10,000	β_2	>10,000	$GABA_A$	>10,000	NET	>10,000
5-HT_{5A}	>10,000	β_3	>10,000	$GABA_B$	>10,000	SERT	>10,000
5-HT_6	>10,000	BZP	9,626 ± 2,385	H_1	>10,000	σ_1	8,232 ± 1,439
5-HT_7	>10,000	Ca^{2+} channel	>10,000	H_2	6,617 ± 1,000	σ_2	2,988

K_i determinations, receptor binding profiles, and agonist functional data were provided by National Institute of Mental Health Psychoactive Drug Screening Program, contract HHSN-271-2008-00025-C (NIMH PDSP). See home page of PDSP (http://pdsp.med.unc.edu) for documentation and experimental details. For mean K_i values < 10,000 nM, SEs are given in addition to mean values, with exception of σ_2 (error not determined).

agonist potencies were greater than 100%, compared with dynorphine for DOR; 100%, compared with salvinorin A for KOR; and 100%, compared with DAMGO for MOR, essentially in the same range as reported for its congener PEO (*9*).

Stability Studies

^{18}F-FE-PEO was found to be highly stable in rat blood (>95% intact parent compound after 2 h of incubation). This result indicates that metabolite determination in rat plasma was not confounded by deterioration of the radiotracer in the blood samples.

Autoradiography

Figure 2 depicts the distribution of ^{18}F-FE-PEO in coronal sections of the Lister hooded rat brain at a concentration of 0.4 nM. Figure 2A represents the native binding pattern of the radiotracer, with high binding in the endopiriform nucleus, the shell of the nucleus accumbens, and the anterior cingulate cortex. Less pronounced binding was found in the striatum. After pretreatment with a 1-μM solution of the MOR-selective OR agonist DAMGO, binding was reduced by 61%, 59%, and 42% in the endopiriform nucleus, anterior cingulate cortex, and striatum, respectively. Preincubation with a 10-μM solution of the nonselective OR antagonist naloxone resulted in a global reduction of binding, with binding in the endopiriform nucleus, anterior cingulate cortex, and striatum reduced by 63%, 65%, and 66%, respectively.

^{18}F-FE-PEO Metabolites

Supplemental Figure 19 shows the time course of the parent fraction in blood (n = 3 rats) and the plasma input function together with the metabolite-corrected plasma input function for 1 rat. Despite the presence of metabolites in the blood, no significant metabolite fraction was found in brain tissue (95% ± 7% parent compound).

PET

High V_T values were observed in the thalamus, parts of the striatum, and the frontal cortex (Figs. 3 and 4). The cerebellum appeared to have the lowest V_T of any brain region. With respect to kinetic modeling, blood-based 1TCM did not provide accurate fits to any of the time–activity curves, including the cerebellum, whereas 2TCM provided good fits to all time–activity curves (Fig. 5). V_T values obtained with 2TCM correlated tightly with those from the Logan plot (Fig. 6), as did BP_{ND} values estimated from the respective V_T values using the distribution volume ratio (DVR) − 1, with the cerebellum acting as the reference tissue (R^2 = 0.957; P < 0.001). As the Logan plot does not assume a particular model structure, the high correlation of

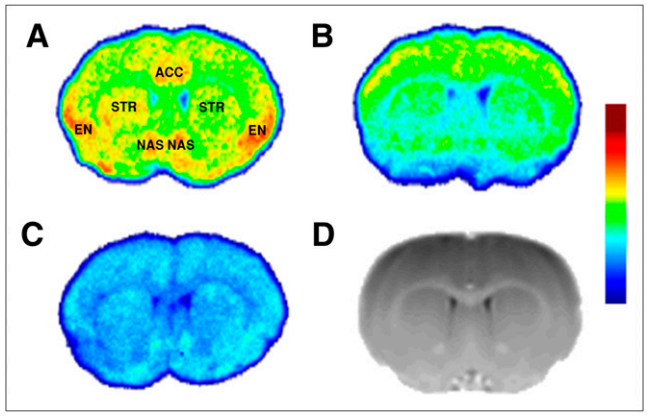

FIGURE 2. Autoradiographic distribution of ^{18}F-FE-PEO in coronal sections of rat brain: without preblockade (A), before incubation with MOR-selective DAMGO (B), and before incubation with nonselective OR antagonist naloxone (C). All autoradiography images have the same absolute intensity range. (D) Coronal section through MR template provides anatomic localization for autoradiography images. ACC = anterior cingulate cortex; EN = endopiriform nucleus; NAS = shell of nucleus accumbens; STR = striatum.

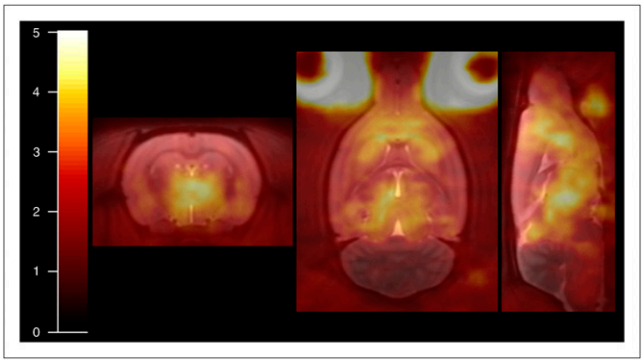

FIGURE 3. Coronal, transverse, and sagittal sections through V_T map for 1 rat overlaid on MR template. V_T map was produced using metabolite-corrected plasma input Logan plot analysis and has color scale threshold of 5.

2TCM V_T estimates with those from Logan plot analysis indicates that although the ligand binds to 3 OR subtypes, the similar affinities mean that kinetically these behave as a homogeneous group and hence can be modeled as a single bound tissue compartment.

Although BP_{ND} values estimated with the reference tissue approaches correlated with those from blood-based modeling, they provided relative underestimates (Fig. 6), likely because of the differential way in which the reference tissue information is used. The failure of 1TCM modeling for the cerebellum (Fig. 5) indicates the presence of nonspecific binding that is kinetically distinguishable from the free compartment and/or specific binding. The latter is likely to be responsible for the relatively poor fits obtained with the reference tissue model and the simplified reference tissue model (Supplemental Fig. 20). In this regard, the reference tissue Logan plot has an advantage over the reference tissue and simplified reference tissue models as it does not assume that the reference tissue can be modeled by a single tissue compartment. It should also be noted that the blood-based BP_{ND} estimates also assume no specific binding in the reference tissue and the same level of nonspecific binding in target and reference regions.

DISCUSSION

Few ^{18}F-labeled ligands have been evaluated and validated for OR imaging (*1,11–14*). Only one of these ligands, ^{18}F-fluorethyldiprenorphine, actually provides subnanomolar affinity (*1*). The main drawback of this radioligand, however, is related to its antagonist properties. Opioid antagonists have shown low susceptibility to changes in endogenous opioid concentration and to challenge with agonist OR ligands (*6*). Hence, because of their higher sensitivity to changes in OR availability, OR agonist ligands are highly desirable, including for our own studies on animal models of drug addiction (*28,29*).

A promising lead for the development of an ^{18}F-labeled agonist OR ligand was published by Marton et al. (*9*). Their orvinol-type full OR agonist (PEO) showed a central nervous system distribution in accordance with OR receptor expression in the rat brain. ^{11}C-PEO PET data acquired in rats indicated a slow pharmacokinetic profile due to high binding affinity to OR sites in the brain (B_{max} (total receptor density)/K_d (dissociation constant) $>$ 1,000 (*9*)). We, therefore, surmised that estimation of V_T and/or BP_{ND} values with acceptable variability from kinetic modeling would require PET data acquisition periods of 3–4 h, and hence the ^{11}C label needed to be replaced by a nuclide with a longer half-life, such as ^{18}F.

A fluorine-labeled analog of ^{11}C-PEO, namely ^{18}F-FE-PEO, was synthesized starting from thebaine, an alkaloid from papaver somniferum. The binding pattern of FE-PEO to a large set of G-protein–coupled receptors, ion channels, and neurotransmitter transporters did not reveal significant off-target binding (Table 1). Despite modification of the lead structure, the binding affinities to cloned human OR remained high; subnanomolar K_i values were found for MOR and KOR and low-nanomolar affinity was observed for DOR. FE-PEO retained full agonist properties, activating DOR, KOR, and MOR with high potency. Based on the in vitro characterization, we conclude that FE-PEO provides promising in vitro characteristics as a full agonist OR ligand.

An automated 2-step process for the production of ^{18}F-FE-PEO was then developed on a TRACERlab FX F-N radiosynthesis module according to the scheme shown in Supplemental Figure 16. The labeling precursor TE-TDPEO was obtained with high chemical purity, and in our initial attempts we used 2 mg of TE-TDPEO. However, the outcome of individual productions was unreliable. Radiochemical yields as high as 30% were accompanied by low-yielding productions with less than 2% product. Hence, the amount of precursor was gradually increased in order to improve the reliability of the automated procedure (Supplemental Fig. 18). Radiochemical yield gradually improved with higher precursor concentration, but more strikingly, so

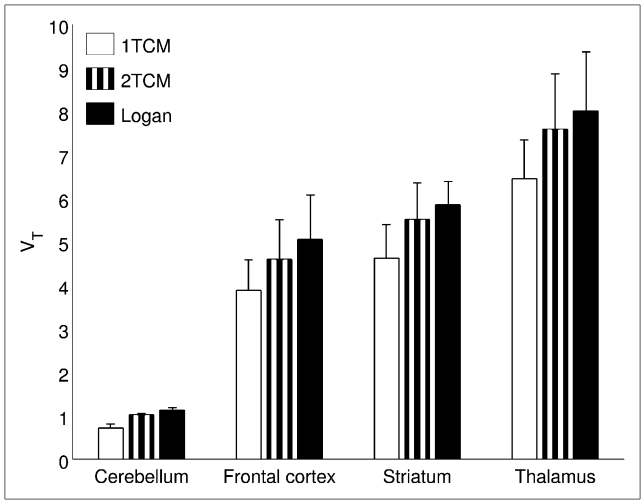

FIGURE 4. Mean regional V_T values (n = 3 scans) produced using metabolite-corrected plasma input in conjunction with 1TCM, 2TCM, and Logan plot analysis. Error bars denote SD.

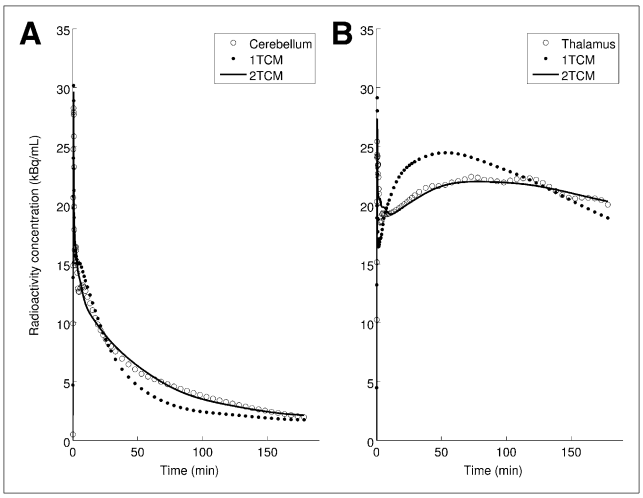

FIGURE 5. Regional time–activity curves for cerebellum (A) and thalamus (B) of 1 scan together with fits to data using metabolite-corrected plasma in conjunction with compartmental modeling with 1 and 2 tissue compartments.

did the consistency of the radiochemical yield, with error margins of less than 3% achieved using greater than 7 mg of TE-TDPEO in 1 mL of MeCN.

However, at this point in the development of ^{18}F-FE-PEO, we observed a general decline of labeling yields. After an approximately 3-mo storage period, radiochemical yield was typically lower than 10% with the formation of an unlabeled by-product. As a result, specific radioactivities of 12–50 GBq/μmol ($n > 20$) at the end of synthesis were obtained in our studies. This apparently low specific radioactivity was attributed to the presence of the nonradioactive by-product, which was found to originate from degradation of the precursor. Exhaustive screening for stationary phase–eluent combinations that permitted separation of the desired radioligand ^{18}F-FE-PEO from this ultraviolet impurity were only partly successful. This problem posed a considerable constraint on our in vivo PET studies, since the exact nature of the by-product was not known and a risk of intoxicating the subject by exposure to a potential OR agonist was possible. However, thorough purification of the precursor by preparative HPLC resulted in a product of sufficient quality for animal studies. Notably, freshly prepared precursor in combination with 2 serial HPLC columns and bombardments of up to 60 min at a proton current of 48 μA resulted in much higher specific activities (52–224 GBq/μmol).

^{18}F-FE-PEO binding (Figs. 2 and 3) was found to be consistent with OR expression data for the rat brain (*3–5*). Autoradiography after preincubation with the nonselective OR antagonist naloxone indicated that nonspecific binding appears to have a relatively uniform distribution (Fig. 2). Pretreatment using the MOR selective agonist DAMGO resulted in a significant reduction in specific binding (>90%) in high-binding regions that express mainly MOR, such as the endopiriform nucleus and anterior cingulate cortex (Fig. 2). Specific binding in the striatum, however, was reduced by approximately 60%. Assuming that DAMGO achieved a high level of occupancy, one can conclude that binding to DOR and/or KOR is a nonnegligible contributor to the specific binding in regions such as the striatum, consistent with the literature (*3–5*). This reduces the effective specificity of ^{18}F-FE-PEO to changes in the MOR system, which is the OR subtype of most interest in addiction and pain processing (*1,9*). Conversion of V_T obtained from blood-based kinetic analysis to DVR−1 in an effort to increase specificity for MOR is compromised by the spatial heterogeneity of the other OR subtypes and perhaps nonspecific binding; otherwise, normalization with V_T in a MOR-devoid area could be a solution. Binding potential estimation from reference tissue modeling is similarly compromised as a MOR-specific measure.

CONCLUSION

The novel radiotracer ^{18}F-FE-PEO was synthesized via an automated process using current good manufacturing practice–compliant equipment. Close similarities in labeling, purification, and quality control facilitate straightforward adoption of ^{18}F-FE-PEO in PET centers that have been using the OR antagonist ^{18}F-fluorethyldiprenorphine. ^{18}F-FE-PEO was obtained in sufficient radiochemical yields and quality for routine application. Binding studies indicated high selectivity for OR compared with other potential targets and full agonist characteristics at all 3 OR subtypes. In vivo evaluation of this OR agonist showed a distribution in accordance with the OR distribution in the rat brain. Quantification of V_T was feasible using metabolite-corrected blood data and is the recommended analysis method. Importantly, no discernible metabolite fraction was found in brain tissue. Reference-tissue Logan plot analysis could be used as an alternative to blood-based kinetic

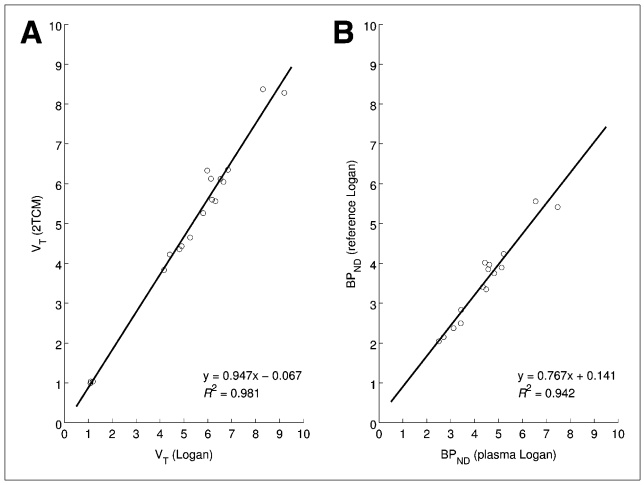

FIGURE 6. Linear regression plots between regional V_T values produced using metabolite-corrected plasma together with Logan plot analysis and 2TCM (A) and regional nondisplaceable BP_{ND} estimated from metabolite-corrected plasma input Logan plot analysis and reference tissue input Logan plot analysis (B). For both plots, statistical significance of Pearson correlation was $P < 0.001$.

analysis. On the basis of the full agonist characteristics and ^{18}F label, we conclude that ^{18}F-FE-PEO is a useful addition to the portfolio of OR imaging agents.

DISCLOSURE

The costs of publication of this article were defrayed in part by the payment of page charges. Therefore, and solely to indicate this fact, this article is hereby marked "advertisement" in accordance with 18 USC section 1734. This study was funded by Medical Research Council (MRC) ICCAM grant G1000018 and by a joint award from the MRC and Wellcome Trust to the Behavioural and Clinical Neuroscience Institute at the University of Cambridge. The study was also supported in part by the Higher Education Funding Council for England (HEFCE), a Rosalie Canney endowed lectureship at the University of Cambridge, the NIMH Psychoactive Drug Screening Program, NIH grant R01 DA017204, and the Wolfson Brain Imaging Centre Major Research Facility. No other potential conflict of interest relevant to this article was reported.

ACKNOWLEDGMENTS

We thank Bianca Jupp, Steve Sawiak, and Carolyn McNabb for their contribution to the biologic evaluation of the radiotracer.

REFERENCES

1. Henriksen G, Willoch F. Imaging of opioid receptors in the central nervous system. *Brain.* 2008;131:1171–1196.
2. Pfeiffer A, Pasi A, Mehraein P, Herz A. Opiate receptor binding sites in human brain. *Brain Res.* 1982;248:87–96.
3. Tempel A, Zukin RS. Neuroanatomical patterns of the μ, δ and κ opioid receptors of rat brain as determined by quantitative in vitro autoradiography. *Proc Natl Acad Sci U S A.* 1987;84:4308–4312.
4. Mansour A, Khachaturian H, Lewis ME, Akil H, Watson SL. Autoradiographic differentiation of mu, delta and kappa opioid receptors in the rat forebrain and midbrain. *J Neurosci.* 1987;7:2445–2464.
5. Mansour A, Khachaturian H, Lewis ME, Akil H, Watson SL. Anatomy of CNS opioid receptors. *Trends Neurosci.* 1988;11:308–314.
6. Hume SP, Lingford-Hughes AR, Nataf V, et al. Low sensitivity of the positron emission tomography ligand [^{11}C]diprenorphine to agonist opiates. *J Pharmacol Exp Ther.* 2007;322:661–667.
7. Frost JJ, Douglass KH, Mayberg HS, et al. Imaging opiate receptors in the human brain by positron tomography. *J Comput Assist Tomogr.* 1985;9:231–236.
8. Hooker JM, Xu Y, Carter P, Schiffer W, Shea C, Fowler JS. Pharmacokinetics of the potent hallucinogen, salvinorin A in primates parallels the rapid onset, short duration of effects in humans. *Neuroimage.* 2008;41:1044–1050.
9. Marton J, Schoultz BW, Hjørnevik T, et al. Synthesis and evaluation of a full-agonist orvinol for PET-imaging of opioid receptors: [^{11}C]PEO. *J Med Chem.* 2009;52:5586–5589.
10. Hjornevik T, Schoultz BW, Marton J, et al. Spinal long-term potentiation is associated with reduced opioid neurotransmission in the rat brain. *Clin Physiol Funct Imaging.* 2010;30:285–293.
11. Schreckenberger M, Klega A, Gründer G, et al. Opioid receptor PET reveals the psychobiologic correlates of reward processing. *J Nucl Med.* 2008;49:1257–1261.
12. Baier B, Bense S, Birklein F, et al. Evidence for modulation of opioidergic activity in central vestibular processing: a [^{18}F] diprenorphine PET study. *Hum Brain Mapp.* 2010;31:550–555.
13. Klega A, Eberle T, Buchholz HG, et al. Central opioidergic neurotransmission in complex regional pain syndrome. *Neurology.* 2010;75:129–136.
14. Mueller C, Klega A, Buchholz HG, et al. Basal opioid receptor binding is associated with differences in sensory perception in healthy human subjects: a [^{18}F]diprenorphine PET study. *Neuroimage.* 2010;49:731–737.
15. Roth BL, Laskowski MB, Coscia CJ. Evidence for distinct subcellular sites of opiate receptors: demonstration of opiate receptors in smooth microsomal fractions isolated from rat brain. *J Biol Chem.* 1981;256:10017–10023.
16. Cheng Y, Prusoff WH. Relationship between the inhibition constant (K1) and the concentration of inhibitor which causes 50 per cent inhibition (I50) of an enzymatic reaction. *Biochem Pharmacol.* 1973;22:3099–3108.
17. Panksepp J, Bishop P. An autoradiographic map of (^{3}H)diprenorphine binding in rat brain: effects of social interaction. *Brain Res Bull.* 1981;7:405–410.
18. Isacson O, Dawbarn D, Brundin P, Gage FH, Emson PC, Björklund A. Neural grafting in a rat model of Huntington's disease: striosomal-like organization of striatal grafts as revealed by acetylcholinesterase histochemistry, immunocytochemistry and receptor autoradiography. *Neuroscience.* 1987;22:481–497.
19. Defrise M, Kinahan PE, Townsend DW, Michel C, Sibomana M, Newport DF. Exact and approximate rebinning algorithms for 3-D PET data. *IEEE Trans Med Imaging.* 1997;16:145–158.
20. Riss PJ, Hong YT, Williamson D, et al. Validation and quantification of [^{18}F] altanserin binding in the rat brain using blood input and reference tissue modeling. *J Cereb Blood Flow Metab.* 2011;31:2334–2342.
21. Gunn RN, Sargent PA, Bench CJ, et al. Tracer kinetic modeling of the 5-HT1A receptor ligand [carbonyl-^{11}C]WAY-100635 for PET. *Neuroimage.* 1998;8:426–440.
22. Innis RB, Cunningham V, Delforge J, et al. Consensus nomenclature for in vivo imaging of reversibly binding radioligands. *J Cereb Blood Flow Metab.* 2007;27:1533–1539.
23. Logan J, Fowler JS, Volkow ND, et al. Graphical analysis of reversible radioligand binding from time-activity measurements applied to [N-^{11}C-methyl]-(−)-cocaine PET studies in human subjects. *J Cereb Blood Flow Metab.* 1990;10:740–747.
24. Hume SP, Myers R, Bloomfield PM, et al. Quantitation of carbon-11-labeled raclopride in rat striatum using positron emission tomography. *Synapse.* 1992;12:47–54.
25. Lammertsma AA, Hume SP. Simplified reference tissue model for PET receptor studies. *Neuroimage.* 1996;4:153–158.
26. Logan J, Fowler JS, Volkow ND, Wang GJ, Ding YS, Alexoff DL. Distribution volume ratios without blood sampling from graphical analysis of PET data. *J Cereb Blood Flow Metab.* 1996;16:834–840.
27. Gunn RN, Lammertsma AA, Hume SP, Cunningham VJ. Parametric imaging of ligand-receptor binding in PET using a simplified reference region model. *Neuroimage.* 1997;6:279–287.
28. Belin D, Dalley JW. Animal models of addiction. In: Verster J, Brady K, Galanter M, Conrod P, eds. *Drug Abuse and Addiction in Mental Illness: Causes, Consequences and Treatment*. Totowa, NJ: Humana Press. In press.
29. Virdee K, Cumming P, Caprioli D, et al. Applications of positron emission tomography in animal models of neurological and neuropsychiatric disorders. *Neurosci Biobehav Rev.* 2012;36:1188–1216.